Thermal transport in dimerized harmonic lattices: Exact solution, crossover behavior, and extended reservoirs

Chih-Chun Chien,[1,*] Said Kouachi,[2] Kirill A. Velizhanin,[3] Yonatan Dubi,[4] and Michael Zwolak[5,†]

[1]*School of Natural Sciences, University of California, Merced, California 95343, USA*
[2]*Department of Mathematics, Qassim University, Al-Gassim, Buraydah 51452, Saudi Arabia*
[3]*Theoretical Division, Los Alamos National Laboratory, Los Alamos, New Mexico 87545, USA*
[4]*Department of Chemistry and the Ilse Katz Institute for Nanoscale Science and Technology,*
Ben-Gurion University of the Negev, Beer-Sheva 84105, Israel
[5]*Center for Nanoscale Science and Technology, National Institute of Standards and Technology, Gaithersburg, Maryland 20899, USA*

We present a method for calculating analytically the thermal conductance of a classical harmonic lattice with both alternating masses and nearest-neighbor couplings when placed between individual Langevin reservoirs at different temperatures. The method utilizes recent advances in analytic diagonalization techniques for certain classes of tridiagonal matrices. It recovers the results from a previous method that was applicable for alternating on-site parameters only, and extends the applicability to realistic systems in which masses and couplings alternate simultaneously. With this analytic result in hand, we show that the thermal conductance is highly sensitive to the modulation of the couplings. This is due to the existence of topologically induced edge modes at the lattice-reservoir interface and is also a reflection of the symmetries of the lattice. We make a connection to a recent work that demonstrates thermal transport is analogous to chemical reaction rates in solution given by Kramers' theory [Velizhanin *et al.*, Sci. Rep. **5**, 17506 (2015)]. In particular, we show that the turnover behavior in the presence of edge modes prevents calculations based on single-site reservoirs from coming close to the natural—or intrinsic—conductance of the lattice. Obtaining the correct value of the intrinsic conductance through simulation of even a small lattice where ballistic effects are important requires quite large extended reservoir regions. Our results thus offer a route for both the design and proper simulation of thermal conductance of nanoscale devices.

I. INTRODUCTION

It is widely known that thermal conduction through translationally invariant harmonic lattices violates Fourier's law due to ballistic transport of phonons through the lattice, which gives a constant thermal conduction versus length rather than a constant conductivity [1–3]. In recent years, however, there has been a tremendous amount of interest in thermal transport in nanoscale systems [4,5], where there is an interplay between ballistic transport, disorder, and diffusion, which requires a deep understanding of not only scattering mechanisms but also transport in—and simulation of—harmonic lattices themselves. Moreover, many technologies require us to harness, control, and understand heat at the nanoscale. This has reached its ultimate expression in the field of phononics, which aims to bring device functionality to thermal transport [6,7], and in the use of thermal transport to characterize nonlinearity in biomolecules [8,9].

One of the main approaches in theoretically investigating thermal transport uses Langevin equations (reviewed in, e.g., Refs. [2,3,6]). In this approach, the system under consideration (described by a given Hamiltonian) is connected to Langevin reservoirs held at different temperatures, which drives heat through the system. The resulting stochastic equations are typically solved numerically, with the thermal current and other properties (temperature profiles, etc.) extracted via time-averaged correlation functions.

When Langevin reservoirs are connected to the two ends of a uniform harmonic lattice, the thermal conductance can be calculated exactly, as demonstrated in Ref. [10]. Generalizing this technique to periodic harmonic lattices with more than a single site or atom per unit cell is an important open problem covering, e.g., nanostructures built from polymers. For instance, phononic devices could employ spatial patterns of DNA bases to tune the operating temperature of a molecular thermal switch based on denaturation [9], which makes use of the different masses, stacking interactions, and hydrogen bonding in DNA [11,12]. This is a physical scenario that goes well beyond phononics, and is relevant to probing fluctuations at the nanoscale, sensing, and device applications [8,13,14].

Here, we develop a method for exactly calculating thermal transport in harmonic lattices with alternating masses, on-site frequencies, and nearest-neighbor couplings when placed between two Langevin reservoirs at the boundary. An exact solution for the thermal conductance in lattices with alternating masses has only recently been found [15,16]. The methods of Refs. [10,15,16], however, rely on a matrix decomposition that does not apply to alternating nearest-neighbor couplings. Here, we utilize some recently developed techniques for diagonalizing analytically a class of tridiagonal matrices [17,18] to construct a unified framework for obtaining exact analytic expressions for the thermal conductance.

The analytic formulas we provide give insight into how multiband systems, which form from the splitting of the bands in the presence of alternation, conduct heat and what

---

*cchien5@ucmerced.edu
†mpz@nist.gov

parameters control the conductance. We use these expressions to show that when a lattice is connected to reservoirs through a single site, the thermal conductance differs substantially from the intrinsic conductance of the lattice [19]. The origin of this large discrepancy is the interfacial resistance due to the emergence of edge modes, the topological nature of which is discussed in detail elsewhere [20].

These results further support the need for using extended reservoirs [19] in simulations where the quantity of interest is the intrinsic conductance of the lattice rather than the conductance of the complete device (i.e., the conductance including the contact resistance to the external reservoirs). It also simultaneously demonstrates the need for analytic solutions to make deficiencies in numerical methods readily apparent and to calibrate simulations.

The structure of the paper is as follows. In Sec. II, we provide a detailed presentation of the theoretical analysis and method of calculation, with some of the more technical aspects left to the appendices. In Sec. III, we discuss the implications of the analytic formula, focusing on the sensitivity of the thermal conductance to the lattice structure and on the relation between the conductance and the coupling to the reservoir, including the turnover behavior of the conductance [19]. In Sec. IV, we summarize the results and conclude.

II. THEORETICAL ANALYSIS

We follow the basic setup of Refs. [1,10] and consider the generic harmonic lattice with N sites in one dimension and with nearest-neighbor coupling,

$$H = \sum_{j=1}^{N} \left(\frac{m_j}{2} \dot{x}_j^2 + \frac{D_j}{2} x_j^2 \right) + \sum_{j=1}^{N-1} \frac{K_j}{2} (x_j - x_{j+1})^2, \quad (1)$$

and connect two additional sites x_0 and x_{N+1} to the ends that are fixed at zero ($x_{0,N+1} \equiv 0$), which symmetrizes the equations of motion. Sites 1 and N are coupled to independent Langevin reservoirs. We also include an on-site harmonic potential, which is common in many problems of interest, such as fluctuations of DNA bases [8]. We will consider lattices that have two sites or atoms per unit cell and thus the triple of parameters has the pattern $(m_1, D_1, K_1), (m_2, D_2, K_2), (m_1, D_1, K_1), \ldots$ For the coupling to the two fixed sites, x_0 and x_{N+1}, we use $K_0 = K_2$ and K_N as the alternate of K_{N-1}, i.e., either K_1 or K_2 depending on whether the lattice has an odd or even length, respectively. As might be expected, the results will depend on whether the lattice is composed of an odd or even number of sites, a fact that we will come back to repeatedly. At the end of the calculation, the thermodynamic limit $N \to \infty$ will be taken while simultaneously preserving the lattice parity (odd or even).

For this setup, the Newton-Langevin equations of motion are

$$m_j \ddot{x}_j = -(D_j + K_{j-1} + K_j) x_j$$
$$+ K_{j-1} x_{j-1} + K_j x_{j+1} + \gamma_j \dot{x}_j + \eta_j, \quad (2)$$

with $\gamma_j = (\gamma_L \delta_{j,1} + \gamma_R \delta_{j,N})$ and $\eta_j = \eta_L \delta_{j,1} + \eta_R \delta_{j,N}$ (Ref. [10] takes $\gamma_{L,R} = \Lambda_{L,R} m_{1,N}$). The left ($L$) and right ($R$) Langevin reservoirs have temperatures T_L and T_R, giving the temperature difference $\Delta T = T_L - T_R$. The random

forces $\eta_{L,R}$ satisfy the fluctuation-dissipation theorem, $\langle \eta_{L,R}(\omega) \eta_{L,R}(\omega') \rangle = 4\pi \gamma_{L,R} T_{L,R} \delta(\omega + \omega')$.

The thermal current (across the whole device, including the interfaces to the external reservoirs) can be calculated from $J = \langle (\gamma_L \dot{x}_1 + \eta_L) \dot{x}_1 \rangle$ using the equations of motion, Eq. (2) [1,10]. In the steady state, the thermal conductance, κ, simplifies to

$$\kappa = \frac{J}{\Delta T} = k_B \gamma_L \gamma_R \int_{-\infty}^{\infty} \frac{d\omega}{\pi} \omega^2 |C_{1N}(\omega)|^2$$
$$\times [(K_{1,N} - \omega^2 \gamma_L \gamma_R K_{2,N-1})^2$$
$$+ \omega^2 (\gamma_L K_{1,N-1} + \gamma_R K_{2,N})^2]^{-1}. \quad (3)$$

Here, $K_{i,j}$ denotes the determinant of the matrix Φ starting from the ith site and ending with the jth site (not to be confused with the single-indexed force constants K_j). k_B is the Boltzmann constant. We note that κ should not to be confused with the thermal conductivity, which is the ratio of the thermal conductance κ and the length of the lattice N in the infinite length limit. Thermal conductivity diverges for the lattices we consider.

The matrix Φ comes from the equations of motion and has a tridiagonal form for one-dimensional (1D), nearest-neighbor harmonic lattices,

$$\Phi = \begin{pmatrix} \alpha_1 & -K_1 & 0 & \cdots \\ -K_1 & \alpha_2 & -K_2 & \cdots \\ & & \ddots & \\ \cdots & 0 & -K_{N-1} & \alpha_N \end{pmatrix}, \quad (4)$$

where

$$\alpha_j = D_j + K_{j-1} + K_j - m_j \omega^2. \quad (5)$$

The quantity $C_{1N}(\omega)$ denotes the cofactor corresponding to the element Φ_{1N}. When the nearest-neighbor coupling is uniform, $K_1 = K_2 = \ldots$, the determinants $K_{i,j}$ can be obtained using a recursion relation [10] $K_{i,j} = \alpha_i K_{i,j-1} - K_i^2 K_{i,j-2}$. For a lattice with uniform $K_j = K$ and alternating on-site parameters, this recursion relation reduces to a product of 2×2 matrices, which gives $K_{i,j}$ and analytic expressions for κ [10,16]. A generalization of that method to nonuniform K_j is not straightforward since there are two alternating recursion relations and a compact expression does not follow. Thus, instead of using the matrix-product method of Refs. [10,16], we will take a different route to obtain analytic expressions for the determinants using trigonometric functions, which then leads to analytic expressions for the thermal conductance. Appendix A gives additional technical details.

Before presenting the analytic expressions, we comment on the effects of the on-site and nearest-neighbor coupling constants. In the continuum limit, the Hamiltonian, Eq. (1) becomes

$$H = \int_0^Z dz \left(\frac{m(z)}{2} (\partial_t x)^2 + \frac{K(z)}{2} (\partial_z x)^2 \right), \quad (6)$$

where z is the longitudinal coordinate and $m(z)$ [$K(z)$] is the local mass [coupling], which may be spatially varying. The on-site coupling D has been included in $K(z)$. Equation (6) suggests that one may interchange the roles of $m(z)$ and $K(z)$ by swapping t and z, replacing spatially varying masses

with spatially varying couplings. However, thermal transport distinguishes the roles of t and z because the inclusion of the two reservoirs at different temperatures breaks the space-time symmetry: In the presence of a steady-state current flowing from the hot reservoir to the cold reservoir, the current is spatially directional. As a consequence, the thermal current in a lattice with alternating couplings is different from one with alternating masses due to the different configurations at the system-reservoir interface. Our approach to the thermal transport applies to the most generic case (including the on-site harmonic potential). Special cases with only alternating masses or only alternating couplings can be readily deduced from the generic case and are presented in Appendix B.

A. Band structure

When both the on-site parameters (masses and on-site frequencies) and the nearest-neighbor harmonic coupling constants are spatially alternating, the conductance can be obtained analytically with the help of the method outlined in Appendix A, which also summarizes recently developed mathematical tools for analytically diagonalizing certain tridiagonal matrices.

Setting

$$\alpha_1 = D_1 + K_1 + K_2 - m_1 \omega^2 \quad (7)$$

and

$$\alpha_2 = D_2 + K_1 + K_2 - m_2 \omega^2, \quad (8)$$

the characteristic polynomial of Φ follows from the condition

$$\alpha_1 \alpha_2 = K_1^2 + K_2^2 + 2 K_1 K_2 \cos(q), \quad (9)$$

which determines the two bands of propagating modes. The determinant can then be found from the characteristic polynomial. The band structure is independent of whether the lattice has an even or odd number of sites as its length scales to infinity. In the presence of the two reservoirs with different temperatures coupled to the ends of the alternating harmonic lattice, however, the thermal conductance is different for even and odd lattices, including in the infinite lattice limit. This is due to boundary effects remaining in this limit for nonequilibrium conditions.

The band structure of an infinite lattice is solely determined by Eq. (9). This gives

$$\cos q = -1 + \frac{1}{2K_1 K_2} \{ m_1 m_2 \omega^4 - [m_1(D_2 + K_1 + K_2) $$
$$+ m_2(D_1 + K_1 + K_2)] \omega^2 $$
$$+ [(D_1 + 2K_1)(D_2 + 2K_2) $$
$$+ (D_1 + 2K_2)(D_2 + 2K_1)]/2 \}. \quad (10)$$

We define $X_{\pm} = (D_2 + K_1 + K_2)/m_2 \pm (D_1 + K_1 + K_2)/m_1$. Then the solution to the constraint is

$$\omega^2 = \omega_{\pm}^2 = \frac{1}{2}[X_+ \pm \sqrt{X_-^2 + U}],$$
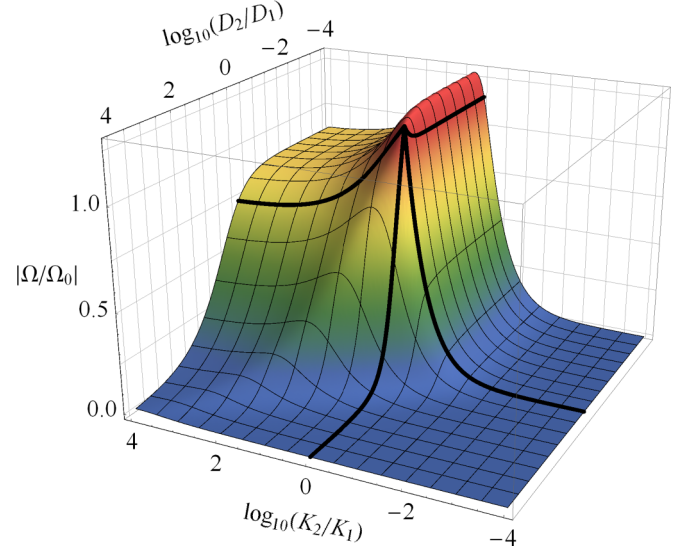$$U = 4\frac{(K_1 - K_2)^2}{m_1 m_2} + 8\frac{K_1 K_2(\cos q + 1)}{m_1 m_2}. \quad (11)$$

FIG. 1. Total bandwidth Ω for harmonic lattices with alternating on-site frequencies (D_2/D_1) and alternating harmonic coupling constants (K_2/K_1). Here, $m_1 = m_2$ and $\Omega_0 = \sqrt{K_1/m_1}$ (K_1 and m_1 are held fixed in the plot). The thick mesh lines mark the lines of uniform coupling constants and uniform on-site frequencies. Note the (relatively shallow) peak in Ω for the uniform lattice.

Since $-1 \leqslant \cos q \leqslant 1$, for positive frequencies, there are two bands $\omega_{+m} \leqslant \omega \leqslant \omega_{+M}$ and $\omega_{-m} \leqslant \omega \leqslant \omega_{-M}$, where

$$\omega_{\pm M} = \sqrt{\frac{1}{2}\left[X_+ \pm \sqrt{X_-^2 + 4\frac{(K_1 \pm K_2)^2}{m_1 m_2}} \right]},$$

$$\omega_{\pm m} = \sqrt{\frac{1}{2}\left[X_+ \pm \sqrt{X_-^2 + 4\frac{(K_1 \mp K_2)^2}{m_1 m_2}} \right]}. \quad (12)$$

The functional form of $\cos q$ and the band structure are symmetric if one swaps either the on-site parameters or the coupling constants. The full symmetry is broken for the thermal conductance [Eqs. (19) and (24), derived in the next section], which only partially respects this symmetry when the couplings to the reservoirs are identical.

The band structure depends on the parameters (m, D, K) of the harmonic lattice (see, e.g., Ref. [19] for a uniform lattice). For the dimerized harmonic lattice, the total bandwidth,

$$\Omega = (\omega_{+M} - \omega_{+m}) + (\omega_{-M} - \omega_{-m}), \quad (13)$$

is shown in Fig. 1 for certain ranges of parameters. The thick mesh lines mark the lines of uniform coupling constants and uniform on-site frequencies. Usually a uniform lattice has the largest total bandwidth in its immediate neighborhood of parameters. However, for the dimerized lattice, there are certain parameter sets that can increase the bandwidth above the uniform lattice, as seen in the figure. In the presence of periodicity, the total bandwidth is thus influenced by all the parameters. For example, when K is uniform and $D_2/D_1 > 1$, Ω increases when $m_2/m_1 > 1$ because a larger mass causes the kinetic energy to offset the larger on-site harmonic potential.

B. Thermal conductance

To obtain the full expression of the thermal conductance, we need the determinant of Φ shown in Eq. (4). If the mass is uniform, one can treat $m\omega^2$ as the eigenvalue of Φ and follow the method described in Appendix A to evaluate it. However, if the masses are alternating with m_1 and m_2, we will use the mass-weighted coordinates $\bar{x}_j = \sqrt{m_j}x_j$ and rewrite the matrix as $\bar{\Phi} = A^T\Phi A$, where A is a diagonal matrix with alternating diagonal elements $1/\sqrt{m_1}$ and $1/\sqrt{m_2}$. The eigenvalues of $\bar{\Phi}$ are ω^2, and the harmonic couplings are rescaled as $K_1/\sqrt{m_1 m_2}$ and $K_2/\sqrt{m_1 m_2}$, respectively. Moreover, $\det(\Phi) = \bar{M}\det(\bar{\Phi})$, where $\bar{M} = (m_1 m_2)^n$ if $N = 2n$ and $\bar{M} = (m_1 m_2)^n m_N$ with m_N denoting the mass of the Nth site if $N = 2n + 1$. Then $\bar{\Phi}$ has the structure described in Appendix A, so the diagonalization method applies. We follow the procedure to find its determinant and eigenvalues and then transform them back to obtain the determinant and eigenvalues of Φ.

We start with the even case, where $N = 2n$ for a positive integer n. The determinants needed for evaluating the conductance are

$$K_{1,N} = (K_1 K_2)^n \frac{\sin[(n+1)q] + (K_2/K_1)\sin(nq)}{\sin(q)},$$

$$K_{1,N-1} = (K_1 K_2)^{n-1}\alpha_1 \frac{\sin(nq)}{\sin(q)},$$

$$K_{2,N} = (K_1 K_2)^{n-1}\alpha_2 \frac{\sin(nq)}{\sin(q)},$$

$$K_{2,N-1} = (K_1 K_2)^{n-1}\frac{\sin(nq) + (K_1/K_2)\sin[(n-1)q]}{\sin(q)}. \tag{14}$$

The cofactor C_{1N} of the present case is independent of ω, and its absolute square is $|C_{1,N}|^2 = (K_1 K_2)^{2(n-1)}K_1^2$. The thermal conductance, Eq. (3), then becomes

$$\kappa = k_B \frac{\gamma_L \gamma_R}{\pi} \int \frac{d\omega \omega^2 K_1^2}{\mathcal{B}_{M1}}, \tag{15}$$

with

$$\mathcal{B}_{M1} = \left(K_1 K_2 \frac{\sin[(n+1)q] + (K_2/K_1)\sin(nq)}{\sin(q)} \right.$$
$$\left. - \omega^2 \gamma_L \gamma_R \frac{\sin(nq) + (K_1/K_2)\sin[(n-1)q]}{\sin(q)}\right)^2$$
$$+ \omega^2(\gamma_R\alpha_1 + \gamma_L\alpha_2)^2\left(\frac{\sin(nq)}{\sin(q)}\right)^2. \tag{16}$$

Following Ref. [10], we treat nq as an independent variable when $n \to \infty$ and average it from 0 to 2π:

$$\int_0^{2\pi} dq\, F(q, nq) \to \int_0^{2\pi} dq \int_0^{2\pi} \frac{dx}{2\pi} F(q, x). \tag{17}$$

With the help of [21]

$$\int_0^{2\pi} \frac{dx}{2\pi}([a\cos(x) + b\sin(x)]^2 + [c\sin(x)]^2)^{-1} = \frac{1}{|ac|}, \tag{18}$$

the final result is

$$\kappa = k_B \frac{2\gamma_L \gamma_R}{\pi} \int_\Omega \frac{d\omega|\omega \sin(q)|}{|\gamma_R\alpha_1 + \gamma_L\alpha_2|\left(\frac{K_2}{K_1} + \frac{\gamma_L\gamma_R}{K_1 K_2}\omega^2\right)}. \tag{19}$$

In Eq. (3) both positive and negative ω are integrated. The domain Ω denotes the bands of positive ω determined by Eq. (9) so a factor of 2 has been included. When $K_1 = K_2$, the result reduces to that of a lattice with alternating masses (for which the expression is shown in Appendix B).

When $\gamma_L = \gamma_R$, Eq. (19) remains the same if one swaps the on-site parameters (so that $\alpha_1 \leftrightarrow \alpha_2$) and keeps the K_j fixed. In contrast, the expression changes if one swaps only K_1 and K_2. In this configuration, the alternating sites show up in pairs—dimers—but there is a harmonic coupling that is unpaired. This is the reason behind this partial symmetry. When $\gamma_L \neq \gamma_R$, this symmetry regarding the on-site parameters is further broken. Ultimately, though, this difference in conductance is due to a topological change in the lattice structure when K_1 and K_2 are swapped. This is discussed in detail in Ref. [20].

Next we study the odd lattice, $N = 2n + 1$ for a positive integer n. The conducting bands are still determined by Eq. (9), but the determinants take on different forms than for the even case:

$$K_{1,N} = (K_1 K_2)^n \alpha_1 \frac{\sin[(n+1)q]}{\sin(q)},$$

$$K_{1,N-1} = (K_1 K_2)^n \frac{\sin[(n+1)q] + (K_2/K_1)\sin(nq)}{\sin(q)},$$

$$K_{2,N} = (K_1 K_2)^n \frac{\sin[(n+1)q] + (K_1/K_2)\sin(nq)}{\sin(q)},$$

$$K_{2,N-1} = (K_1 K_2)^{n-1}\alpha_2 \frac{\sin(nq)}{\sin(q)}. \tag{20}$$

The absolute square of the cofactor is $|C_{1N}|^2 = (K_1 K_2)^{2n}$. The conductance, Eq. (3), is then

$$\kappa = k_B \frac{\gamma_L \gamma_R}{\pi} \int d\omega \frac{\omega^2}{\mathcal{B}_{M2}}, \tag{21}$$

with

$$\mathcal{B}_{M2} = \left(\frac{\alpha_1 \sin[(n+1)q]}{\sin(q)} - \frac{\omega^2 \gamma_L \gamma_R \alpha_2 \sin(nq)}{K_1 K_2 \sin(q)}\right)^2$$
$$+ \omega^2([(\gamma_L + \gamma_R)\sin[(n+1)q]$$
$$+ \left(\frac{K_1}{K_2}\gamma_L + \frac{K_2}{K_1}\gamma_R\right)\sin(nq)]\frac{1}{\sin(q)})^2. \tag{22}$$

Again we treat nq as an independent variable when $n \to \infty$ and average it from 0 to 2π. Using the integral [21]

$$\int_0^{2\pi} \frac{dx}{2\pi}\{[A\sin(x) + B\cos(x)]^2$$
$$+ [C\sin(x) + D\cos(x)]^2\}^{-1} = |CB - AD|^{-1}, \tag{23}$$

the final result is

$$\kappa = k_B \frac{2\gamma_L \gamma_R}{\pi} \int_\Omega d\omega|\omega \sin(q)|\left|\alpha_1\left(\frac{K_1}{K_2}\gamma_L + \frac{K_2}{K_1}\gamma_R\right)\right.$$
$$\left. + \frac{\gamma_L \gamma_R(\gamma_L + \gamma_R)\omega^2\alpha_2}{K_1 K_2}\right|^{-1}. \tag{24}$$
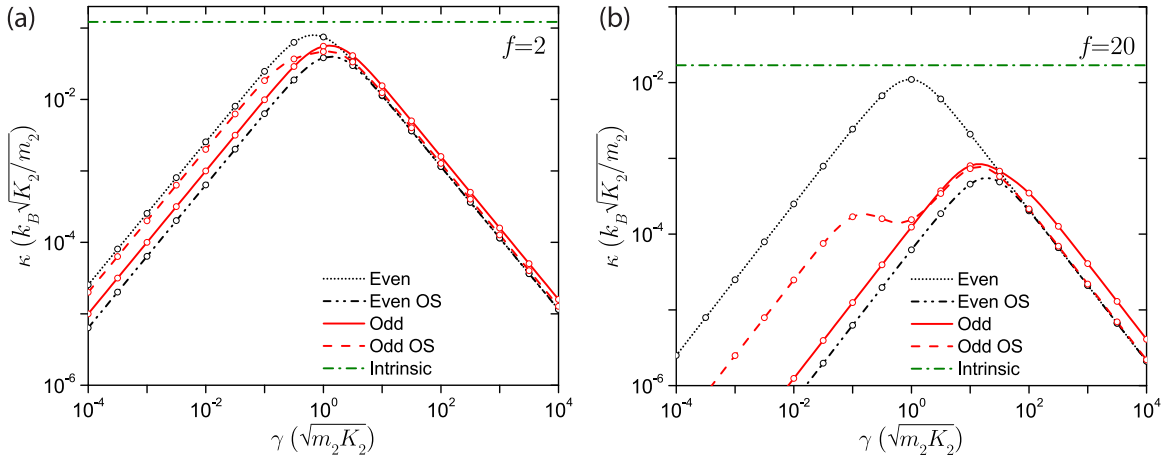
FIG. 2. Thermal conductance, κ, versus γ for even and odd lattices. The parameters are $(m_1/m_2, D_1/D_2, K_1/K_2) = (f, f, f)$ (short dotted black line and solid red line for the even and odd lattices, respectively) and the same set of parameters but with the ordering switched (OS) (dashed lines), so that (m_1, D_1, K_1) changes places with (m_2, D_2, K_2) (dash-dot-dot black line and dashed red line for the even and odd lattices, respectively). (a) The conductance for $f = 2$. All lines correspond to the same set of alternating parameters, i.e., the same bulk properties. The only difference is whether the lattice is of odd or even length and the ordering of the parameters. (b) The conductance for $f = 20$. For small γ, all curves rise linearly with γ, while for large γ they decay as $1/\gamma$. The green dash-dotted line indicates the intrinsic conductance, κ_0 of Eq. (34), which is directly proportional to the bandwidth. Many of the lattice configurations fail to even come close to the intrinsic conductance. The circles are direct numerical simulations on a $N = 128$ length lattice ($N = 129$ for the odd case) following Ref. [19].

The domain of integration Ω only covers positive ω so a factor of 2 is included. When $m_1 = m_2 = m$, this expression reduces to that of a lattice with alternating coupling constants, as shown in Appendix B.

When $\gamma_L = \gamma_R$, swapping K_1 and K_2 keeps the expression intact, but swapping the on-site parameters (so that $\alpha_1 \leftrightarrow \alpha_2$) leads to a different value for the conductance. This partial symmetry is further broken when $\gamma_L \neq \gamma_R$. The bands are fully symmetric when K_1 and K_2 are swapped or α_1 and α_2 are swapped. Thus, the presence of the reservoirs and the thermal current reduces this full symmetry.

The special case of a harmonic lattice with alternating on-site parameters and uniform nearest-neighbor couplings is similar to the even case here. The special case of a harmonic lattice with uniform on-site parameters and alternating near-neighbor couplings is similar to the odd case when the lengths are identical. These cases are summarized in Appendix B

III. DISCUSSION

The setup we considered above consists of a one-dimensional (or quasi-one-dimensional) lattice connected only at its boundaries to thermal reservoirs. Such a setup can be made by examining the low-energy properties of, e.g., an alternating copolymer bonded at its ends to two crystals, which act as the thermal reservoirs. When the thermal reservoirs are well approximated by ohmic, Langevin reservoirs, the equations we derived, Eqs. (19) and (24), give the conductance of the full device, which includes contributions from the contact resistance to the thermal reservoirs. This full device conductance is surprisingly variable even when the Langevin coupling is fixed or otherwise restricted to a limited range (as is often the case), which we will now discuss. Afterward, we will discuss how this relates to the intrinsic conductance of the lattice [19].

A. Full device conductance

Figure 2 shows the conductance of several lattices versus the friction coefficient $\gamma_L = \gamma_R = \gamma$. One can immediately see the expected crossover behavior from a small γ regime, where $\kappa \propto \gamma$, to a large γ regime, where $\kappa \propto 1/\gamma$. This can be readily verified by Eqs. (19) and (24) since both of them have the form $\kappa = \gamma A \int_\Omega d\omega \omega |\sin[q(\omega)]|/|B(\omega) + \gamma^2 C(\omega)|^{-1}$. When $\gamma \to 0$, they become $\kappa \to \gamma A \int_\Omega d\omega \omega |\sin[q(\omega)]/B(\omega)| = C_1 \gamma$. In the other limit when $\gamma \to \infty$, they become $\kappa \to \gamma A \int_\Omega d\omega \omega |\sin[q(\omega)]/[\gamma^2 C(\omega)| = C_2/\gamma$. The coefficients C_1 and C_2 can be obtained by numerical calculations or, as will be shown in Appendix C, analytically.

The underlying physics of this turnover is the same as that described by Kramers' transition state theory: In the small γ regime, the implicit reservoirs are too weakly coupled to the system to effectively pump in energy. In other words, the free lattice—the lattice not connected to Langevin reservoirs—ushers away energy faster than it can be input by the reservoir. In the strong γ regime, the implicit reservoirs are too strongly coupled to the end lattice sites so that they effectively decouple them from the lattice (i.e, friction distorts the natural lattice dynamics creating a mismatch between the sites connected to the reservoirs and the rest of the lattice). Propagating modes that are carrying energy are thus reflected at the interfaces between the free lattice and the sites connected to the reservoirs [19]. These reflections, or recrossings, prevent energy from being transferred into and out of the sites connected to the reservoirs.

The figures, though, also show a surprising feature: Lattices that are equivalent in terms of their phonon bands can give a drastically different conductance. Figure 2(a), for instance, plots the conductance for the same lattice parameters $(m_1/m_2, D_1/D_2, K_1/K_2) = (f, f, f)$ with $f = 2$ except in four different configurations: An even lattice, an odd lattice, and even (odd) lattices but with the ordering of parameters switched, "OS", i.e., the oscillator masses for these

four cases are $[m_1, m_2, m_1, \ldots, m_2]$, $[m_1, m_2, m_1, \ldots, m_2, m_1]$, $[m_2, m_1, m_2, \ldots, m_1]$, and $[m_2, m_1, m_2, \ldots, m_1, m_2]$, respectively (all other parameters change in a similar way). All these lattices have the same phonon bands. Yet, in the small γ regime, the conductance differs by a factor of 4. Figure 2(b), which uses $f = 20$, shows a variation in conductance by almost three orders of magnitude for the same four configurations. These differences can be made even more dramatic when lattices with the same phonon bands but different parameters are considered [i.e., the bands, Eq. (12), are identical under the change f to $1/f$. Yet, this changes the conductance via an effective change in the coupling γ]. We remark that the OS cases are not equivalent to a simple swap of the two reservoirs. In exchanging the alternating parameters, the nearest-neighbor couplings at the system boundary also change, e.g., from K_2 to K_1.

Indeed, some of this difference is expected. Considering, for instance, the Casher-Lebowitz formula for a uniform lattice with parameters (m, D, K), in the infinite-length limit one can show that [19]

$$\kappa = \frac{k_B \gamma}{2m} \tag{25}$$

in the small γ regime. This indicates that when changing the mass of the lattice site connected to the Langevin reservoir, the conductance should change. When altering the configuration, for instance, from even to odd (i.e., the masses go from $[m_1, m_2, m_1, \ldots, m_2]$ to $[m_1, m_2, m_1, \ldots, m_2, m_1]$, and similarly for other parameters), the conductance should change as we have two m_1 masses connected to the reservoirs instead of one m_1 and one m_2. This, however, will only account for at most an order of magnitude of the differences observed above. Thus, there is yet another physical effect that is resulting in these large differences for lattices that have equivalent phonon bands. Before revealing this effect, we will first develop a quantitative description of the small γ regime, which will allow us to describe the drastic differences in the conductance.

B. Small γ conductance

For small γ, the lattice can be thought of as independent phonon modes, as any correlations induced by the reservoirs will be higher order in γ. Moreover, just as with Kramers' theory and the lattices examined in Ref. [19], this regime reflects that the modes are removing energy away from the interface faster than it can be restored by the reservoir, and thus the conductance (or current) is controlled completely by the rate of heat input into that mode from the reservoir, i.e., by the effective coupling of the reservoirs to the mode.

Defining an effective coupling to the left, $\tilde{\gamma}_{qL}$, and right, $\tilde{\gamma}_{qR}$, reservoirs for each mode, we can understand this regime in a very simple fashion from the stochastic nature of the reservoir: The energy input from the left reservoir into mode q is $J_{qL} = k_B \tilde{\gamma}_{qL}(T_L - T_q)$ and from the right $J_{qR} = -k_B \tilde{\gamma}_{qR}(T_R - T_q)$, where the minus sign just reflects that we want the right moving current on both ends. In the steady state, $J_{qL} = J_{qR} = J_q$. Using this to eliminate the unknown quantity T_q (the temperature of mode q), we find

$$J_q = k_B \left(\frac{\tilde{\gamma}_{qL} \tilde{\gamma}_{qR}}{\tilde{\gamma}_{qL} + \tilde{\gamma}_{qR}} \right) \Delta T \equiv \kappa_q \Delta T, \tag{26}$$

where κ_q is the conductance of mode q. We note that the effective rate that matters for the thermal current (or conductance) in this regime is the reduced, effective γ.

The effective reservoir coupling will depend on the weight of the mode on the left or right end sites:

$$\tilde{\gamma}_{qL} = \gamma_L u_{q1}^2, \quad \tilde{\gamma}_{qR} = \gamma_R u_{qN}^2, \tag{27}$$

where u_{qn} are the real-valued polarization vectors for the normal mode q at site n, $= 1, \ldots, N$. Given $H = \frac{1}{2} \mathbf{p}^\intercal \mathbf{M}^{-1} \mathbf{p} + \frac{1}{2} \mathbf{x}^\intercal \mathbf{K} \mathbf{x}$, $u_{qn} = [\mathbf{M}^{-1/2} \mathbf{T}]_{nq}$, where $\mathbf{T}$ is the orthogonal transformation that diagonalizes the mass-weighted coupling matrix $\mathbf{M}^{-1/2} \mathbf{K} \mathbf{M}^{-1/2}$.

Essentially, Eq. (26) indicates that the conductance for each mode is given by two resistors in series,

$$\frac{k_B}{\kappa_q} = \frac{1}{\gamma_L u_{q1}^2} + \frac{1}{\gamma_R u_{qN}^2}, \tag{28}$$

reflecting the resistance at the two contacts and the (relatively) negligible resistance of the bulk lattice. The total conductance is then given by

$$\kappa = \sum_q \kappa_q. \tag{29}$$

We give a rigorous derivation of these formulas in Ref. [20]. We note that Eqs. (26) and (29) yield some of the expressions in Ref. [22].

For instance, for a uniform lattice with parameters (m, D, K), the polarization vector is given by

$$u_{qn} = \sqrt{\frac{2}{m(N+1)}} \sin(nq), \tag{30}$$

where $q = k\pi/(N+1)$ for $k, n = 1, \ldots, N$ for a finite length lattice. For the coupling to the right reservoir (at site N), we use that $\sin[Nk\pi/(N+1)] = \sin[(N+1) - 1)k\pi/(N+1)] = -\sin[1k\pi/(N+1)]$. Taking Eq. (30) and the continuum limit, one obtains for Eq. (29)

$$\kappa \approx \frac{2k_B \gamma}{m\pi} \int_0^\pi dq \frac{\sin(q)^2 \sin(q)^2}{\sin(q)^2 + \sin(q)^2} = \frac{k_B \gamma}{2m}, \tag{31}$$

which is exactly the Casher-Lebowitz formula in this limit. Since we worked with the finite lattice modes, Eq. (30), q goes from 0 to π. We can replace $2\int_0^\pi \to \int_0^{2\pi}$ if desired.

Equation (29) is exact for the conductance in the small γ regime. Since it is a linear sum of the contribution of each mode, it can be separated into total contributions from each of the two bands. Figure 3 shows κ and Eq. (29) separated into the individual band contributions. The linear regime in the cases shown is dominated by one of the two bands. Essentially, this is due to the large differences in masses, as discussed in the figure caption. We note that features observable in the conductance versus γ are due to the distinct contributions of each of the bands and when they turn over into the large γ regime. We further discuss the small (and large) γ regimes in Appendix C.

We are now in a position to understand why there is such a drastic difference between the conductance of lattices that one might expect to be identical. One effect is due to the different masses, as mentioned above. It is clear from the form of the
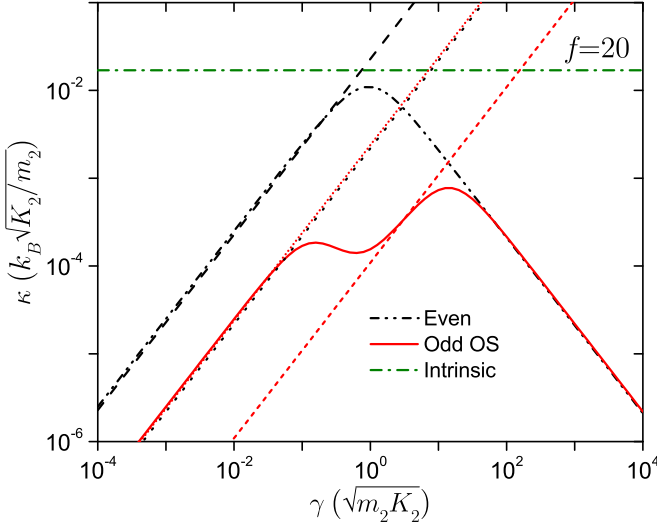
FIG. 3. The band-delineated conductance in the small γ regime. The three lines in the legend show the conductance for $(m_1/m_2, D_1/D_2, K_1/K_2) = (f, f, f)$ with $f = 20$. The remaining lines show Eq. (29) divided into the contributions from each band for a finite lattice with $N = 128$ (dashed and dotted black lines) and $N = 129$ (short dotted and short dashed red lines). Since Eq. (29) is linear, each normal mode contributes separately to the conductance. Each band has a majority and minority sublattice, where most of the mode amplitude (the local masses times the polarization vector) is on the majority lattice. For even lattices, both bands have a direct connection to the Langevin reservoirs. However, one band has a majority lattice that has a larger mass, and therefore the polarization vector—the quantity that determines the contribution to the conductance for small γ—is more balanced, i.e., u_{q1}^2 and u_{qN}^2 are similar in magnitude (For example, when the odd sublattice is the majority sublattice and $m_1 \gg m_2$, then $m_1 u_{q1}^2 \gg m_2 u_{qN}^2$, but u_{q1}^2 is of the same order as u_{qN}^2). The other band—the higher frequency band—has a majority amplitude on the small mass sublattice, which means its polarization vector on the large mass sublattice is further suppressed (i.e., multiplied by the inverse of the large mass). This leads to a large imbalance in u_{q1}^2 and u_{qN}^2 and the weaker of the two dominates the conductance, decreasing its magnitude. For odd lattices, one band is connected at both ends to the Langevin reservoirs, whereas the other band is only connected through its minority sublattice. Thus, not only is there a splitting of the contribution of the two bands, but the high-frequency band can be the dominant contribution at small γ. The turnover occurs earlier for this band, and later for the band only indirectly coupled to the Langevin reservoirs, which gives a two-peak structure to the conductance versus γ.

effective coupling coefficients, Eq. (27), that this can not be the only effect: The orthogonal transformation **T** will by definition have all its matrix elements on, e.g., site n sum to 1 when squared (likewise, the polarization vectors when summed over q at a particular site n have to sum to the inverse mass at that site). Thus, the modes present and their weight at the end sites (which are in contact with the reservoirs) play a crucial role.

C. Role of edge modes

The large variability of the conductance—even for lattices with the same bulk properties—is due to the formation of edge modes, the appearance of which is determined by the configuration of the lattice. The edge modes are states that have a fre-

quency within the phonon band gap, and consequently decay exponentially away from the interface. Their coupling to one of the reservoirs is large and the other exponentially small, and [in light of Eq. (29)] this will have an effect on the thermal conductance. This will not be a trivial effect, i.e., zero contribution from 1 or 2 modes out of the (thermodynamically) large number of modes N. Rather, the edge modes will deplete the couplings of the other modes to the Langevin reservoirs, therefore reducing the conductance. Edge modes appear in other physical contexts, see, e.g., Refs. [23,24]. Their topological origin is discussed in Ref. [20]. Here, we will limit the discussion to the effect of these modes on the conductance and, then, how extended reservoir simulations can correctly obtain the bulk, or intrinsic, conductance even when these modes are present.

For any harmonic lattice, we have the sum rules

$$\sum_q u_{qn}^2 = \frac{1}{m_n} \tag{32}$$

for each site n. The sum here is over all modes, edge or otherwise. The sum rules come from the transformation of the mass-weighted coordinates to normal modes, where the orthogonal transformation matrix has each column or row normalized to 1. Returning to the original coordinates gives the sum rules.

By definition, a localized mode is one that has a large amplitude on a particular site or region of sites. This means that u_{qn}^2 will be large and roughly independent of N, i.e., it will not depend on the lattice length. This will deplete the amplitude of all other modes, as now instead of summing to $\frac{1}{m_n}$, they will sum to $\frac{1}{m_n} - \sum_{q \in \mathcal{E}} u_{qn}^2$, where $\mathcal{E}$ is the set of all localized (or, as is the case here, edge) modes.

To give a more detailed example, one should look at the eigenvalues of Φ in Eq. (4), which can be determined by the technique summarized in Appendix A. We focus on the case when only the nearest-neighbor couplings alternate (so that $m_1 = m_2 = m$ and $D_1 = D_2 = D$). When the lattice is semi-infinite in length with the left boundary open, in addition to the delocalized modes, there is also a normal mode with amplitude $\propto (1, 0, (-K_1/K_2), 0, (-K_1/K_2)^2, \ldots)$ from the left edge (and potentially from the right edge as well). So long as the lattice is long enough, one need not worry about interaction between the edges). This mode decays with exponent $\xi = -\ln(K_1/K_2)$ and thus only exists when $K_1 < K_2$. Properly normalizing and mass weighting, this yields $u_{q1}^2 = [1 - (K_1/K_2)^2]/m$, leaving a total of

$$\sum_{q \in \Omega'} u_{qn}^2 = \frac{1}{m} \left(\frac{K_1}{K_2} \right)^2 \tag{33}$$

to contribute to the effective coupling of the delocalized modes to the Langevin reservoir at the left. The quantity Ω' designates the bands of the propagating phonon modes, i.e., $q \in \Omega'$ excludes the edge mode. In other words, the presence of the edge modes can drastically deplete the coupling of the remaining modes to the reservoir. For the examples shown in Fig. 2, for instance, changing the configuration from one where $K_1 > K_2$ (short dotted black lines) to one with $K_1 < K_2$ (dash-dot-dot black lines, i.e., the parameters all swapped), introduces two edge modes (note that the thermal conductance is always computed with N finite, and then limit $N \to \infty$ is

taken at the end of the calculation, so there are always two open boundaries). The conductance drops by exactly a factor of $f^2 = (K_1/K_2)^2$ (or 4 and 400 for the parameters in that figure). Moreover, note that when swapping the parameters for $\gamma_L = \gamma_R = \gamma$ and N even, there is no trivial mass effect as discussed above, as one has an m_1 mass on one side and an m_2 mass on the other in both cases.

When the lattice is odd in length, there is always one edge mode, either at the left or right edge. In addition to the trivial mass effect, there is also a nontrivial suppression of the conductance similar to the even length case (full expressions can be found in Appendix C). Outside of the linear regime, there is intricate behavior of the conductance—sometimes including a minimum in its value versus γ—due to the nontrivial change in which band is directly connected to both reservoirs through its majority lattice, as discussed in the Fig. 3 caption.

The physical effect of structural configurations on the conductance can be used in the design of nanoscale devices that rely on thermal transport. For instance, simply discarding (or adding) a monomer of an alternating copolymer ($A - B - A - B - A - B - A \rightarrow B - A - B - A - B - A$) can significantly change the conductance. Moreover, this effect can be used in tandem with nonlinearity, as was proposed in Ref. [9]. Exploiting, e.g., more complicated copolymers and the ability to alter the ends separately from the bulk of the lattice, one can introduce or remove edge modes, seeing in practice the large changes observed here. These results suggest that the tuning structural parameters and configurations give a powerful method to engineer thermal transport. The suppression of thermal conductance here is not a reflection of thermal rectification, where nonlinearity or multiband effects are usually required [25]. The emergence of localized modes reduces the coupling between the reservoirs and the conducting modes, so only reversing the two reservoirs does not lead to rectification. Our results are consistent with previous studies showing that classical harmonic systems do not exhibit thermal rectification [25–28].

D. Intrinsic conductance

We have seen above that when contacting the system at just the boundaries, the conductance is highly sensitive to the configuration of the lattice, even when the bulk properties do not change. Another bulk property is the intrinsic conductance of the lattice. For a harmonic system, the intrinsic thermal conductance is determined by the maximum rate at which the lattice can conduct heat when placed between two thermal reservoirs in equilibrium [19]: When two lattices initially disconnected and in equilibrium at different temperatures are connected, the thermal current flowing from left to right is $J_{L \to R} = k_B T_L l_L^{-1} \sum_{q>0} v_q$, where v_q is the group velocity of a phonon with momentum $q > 0$ and l_L is the length of the left lattice. Similarly for the current flowing from right to left. When taking the infinite lattice limit, one finds [19]

$$\kappa_0 = \frac{k_B \Omega}{2\pi}, \tag{34}$$

where Ω is the total bandwidth (note we use Ω to designate both the bandwidth and the bands). From this expression and the analytic form for Ω derived in the previous section, Eq. (13), one can obtain the conductance for the lattice only (without
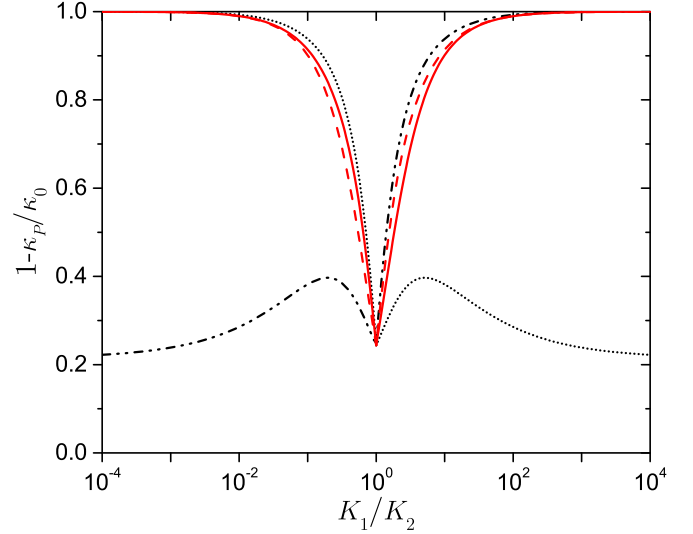

FIG. 4. The relative difference between the peak thermal conductance (versus γ) and the intrinsic conductance versus $K_1/K_2 = f$. All four lattices are shown (the short dotted black line shows the even lattice, the dash-dot-dot black line the even lattice with the parameters swapped, the solid red line the odd lattice, and the dashed red line the odd lattice with the parameters swapped). The parameters are $(m_1/m_2, D_1/D_2, K_1/K_2) = (f, f, f)$. This shows that there is a nonlinear relation between the conductance of a system with only its boundaries attached to thermal reservoirs and the intrinsic conductance of the lattice only. When the relative difference between these two quantities is $\mathcal{O}(1)$, it means that κ_P is negligibly small compared to κ_0. Often the intrinsic conductance is the desired quantity, as a particular device setup is not of interest, but rather, e.g., scaling properties of the lattice conductance with length, nonlinearity, etc. This shows that contacting the lattice at the boundary can not achieve this result.

contact effects). The bandwidth (or intrinsic conductance times 2π) is shown in Fig. 1. Note that for more intricate systems, such as nanoscale devices where both diffusive and ballistic transport play a role, the intrinsic conductance is defined as the lattice conductance in the absence of contact effects.

When considering the whole system, including the contacts to the reservoirs, the conductance always has to be lower due to a contribution to the resistance from the contacts (which will depend on γ). The behavior of the conductance in the small and large γ regimes thus leads to a peak in the conductance, $\kappa_P < \kappa_0$, at the crossover. The periodicity, however, significantly alters κ_P. Indeed, for some configurations of the lattice, as we have seen, there are edge modes at the interface. Thus, there is no reason to expect that κ_P will ever get close to κ_0. Figure 4 plots the relative difference

$$\frac{\kappa_0 - \kappa_P}{\kappa_0}, \tag{35}$$

which can be seen as a measure of the simulation fidelity when trying to extract the intrinsic conductance without an adequate treatment of contact effects. The peak conductance differs drastically from the intrinsic conductance for essentially all parameters. Only for the lattice without edge modes (all configurations at $K_1 = K_2$ or the even length lattice where the weaker bonds contact the hard wall) does it come reasonably close (but still off by about 20 %).
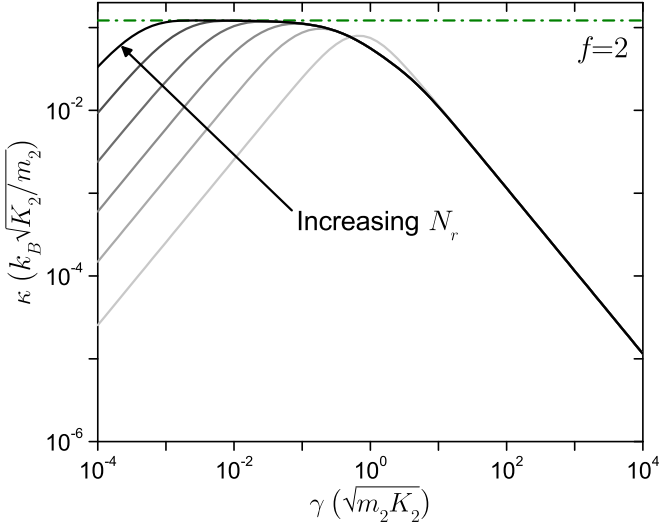
FIG. 5. Thermal conductance, κ, versus γ for an even lattice with a free lattice length of 128 and $(m_1/m_2, D_1/D_2, K_1/K_2) = (f, f, f)$ with $f = 2$. The lines show different extended reservoir lengths, $N_r = 1, 4, 16, 64, 256, 1024$. The green dash-dotted line indicates the intrinsic conductance, κ_0 of Eq. (34). The extended reservoirs ensure the development of a plateau region at the intrinsic conductance of the lattice. This allows the extraction of the intrinsic conductance of the lattice from numerical simulations.

Previously, we demonstrated that extended reservoirs allow one to extract the intrinsic conductance of the lattice of interest [19]. Extended reservoirs are regions of length N_r on each end of the lattice, where all the sites in the region are connected to Langevin reservoirs. This allows γ to be very weak while pumping in sufficient energy to ensure that the free lattice—the lattice of interest—limits the conductance. The use extended reservoirs results in the formation of a plateau in the conductance versus γ, where the plateau conductance is the intrinsic conductance.

Figure 5 shows the development of a plateau region as N_r is increased for a configuration without edge modes. Clearly,

the intrinsic conductance for this system can be accurately calculated via this simulation approach. However, above we saw that the different configurations had drastically different behavior (both qualitatively and quantitatively). Figure 6 shows the plateau formation for $f = 2$ and $f = 20$ for all the configurations (even, odd, even OS, odd OS). Indeed, the extended reservoirs wash out the effect of the edge modes and other boundary effects, allowing the computed conductance to plateau at the intrinsic conductance of the lattice. While requiring reasonably large extended reservoir regions, this demonstrates the power of the simulation approach for determining the intrinsic conductance of a lattice of interest, rather than a full device configuration (where the interfaces are approximated by Langevin reservoirs, opposed to the actual, atomically detailed interface). In Ref. [19], we demonstrated that this plateau behavior applies to nonlinear systems, where both diffusive and ballistic effects are present.

IV. CONCLUSION

We derived a compact, exact analytic expression for the thermal conductance of a harmonic lattice with alternating on-site and nearest-neighbor coupling constants. The derivation is based on a recently developed method for diagonalizing a class of tridiagonal matrices. This approach is different from the methods of Refs. [10,15,16] and allows one to explore inhomogeneous couplings. Moreover, this approach may be generalized to more complicated periodicity. We used the analytic expressions to examine the effects of on-site parameters and nearest-neighbor couplings, as well as the boundaries, in determining the thermal conductance. The results clarify the effect of the reservoirs on the conductance, which is more complex when the lattice is not uniform. This intricate behavior is mainly due to the presence of an interfacial resistance due to edge modes in the alternating lattice. Their topological origin is discussed in Ref. [20]. Moreover, the findings presented here support the use extended reservoirs to compute the thermal conductance.
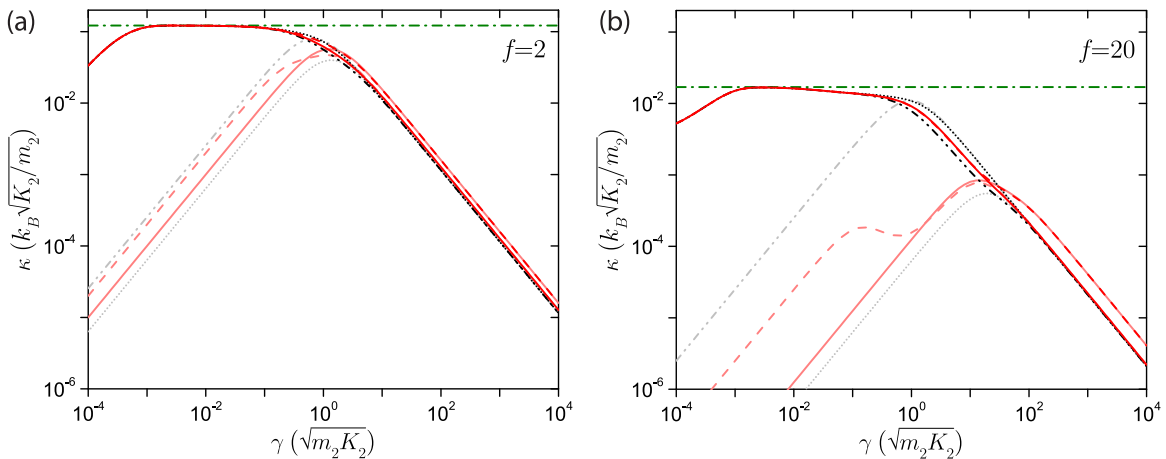

FIG. 6. Thermal conductance, κ, versus γ for an even lattice with a free lattice length of 128 (or 129) and $(m_1/m_2, D_1/D_2, K_1/K_2) = (f, f, f)$ with $f = 2$ and $f = 20$. The short dotted black line and solid red line are for the even and odd lattices, respectively, and the dash-dot-dot black line and dashed red line are for the even and odd lattices with the parameters switched, respectively. Lighter lines show single site reservoir regions, $N_r = 1$, and darker lines, $N_r = 1024$. (a) For $f = 2$, the plateau forms and washes out differences in the conductance due to the configuration. (b) For $f = 20$, a plateau starts to form and washes out configuration effects.

APPENDIX A: EIGENVALUES OF A CLASS OF TRIDIAGONAL MATRICES

We consider the following types of tridiagonal matrices (N is a positive integer, which in the main text represents the total number of sites)

$$A_N = \begin{pmatrix} b_1 & a_1 & 0 & ... & 0 \\ c_1 & b_2 & a_2 & 0 & ... \\ 0 & c_2 & b_1 & a_1 & 0 \\ \vdots & \ddots & c_1 & \ddots & \ddots \\ 0 & \cdots & 0 & \ddots & b_N \end{pmatrix}, \quad (A1)$$

where $a_i, b_i, c_i, i = 1,2$ are complex numbers. To simplify the notation, we consider

$$a_1 c_1 = d_1^2 \quad \text{and} \quad a_2 c_2 = d_2^2. \quad (A2)$$

The matrices studied in Refs. [29–32] are special cases of those considered by Kouachi [17,18] and here we further generalize the formalism to matrices with alternating diagonal and band-diagonal elements.

The forms of the characteristic determinant Δ_N^0 of the class of matrices A_N depends on whether N is odd ($N = 2n + 1$) or even ($N = 2n$)

$$\begin{cases} \Delta_{2n+1}^0 = (d_1 d_2)^n Y_1 \frac{\sin(n+1)\theta}{\sin\theta}, \\ \Delta_{2n}^0 = (d_1 d_2)^n \frac{\sin(n+1)\theta + \frac{d_2}{d_1}\sin(n\theta)}{\sin\theta}, \end{cases} \quad (A3)$$

with

$$Y_1 = b_1 - \lambda, Y_2 = b_2 - \lambda. \quad (A4)$$

Here, λ denotes the eigenvalue that will be found. By expanding Δ_N^0 in terms of its last column and using Eqs. (A2) and (A4), we get

$$\Delta_N^0 = \begin{cases} Y_1 \Delta_{N-1}^0 - d_2^2 \Delta_{N-2}^0, & \text{when } N = 2n+1, \\ Y_2 \Delta_{N-1}^0 - d_1^2 \Delta_{N-2}^0, & \text{when } N = 2n. \end{cases} \quad (A5)$$

We begin by proving the second line of Eq. (A3). By writing the expressions of Δ_N^0 for $N = 2n + 2, 2n + 1$ and $2n$, respectively, multiplying Δ_{2n+1}^0 and Δ_{2n}^0 by Y_2 and $(d_1 d_2)$, respectively, and adding the three resulting equations, we get

$$\Delta_{2n+2}^0 = \left[Y_1 Y_2 - \left(d_1^2 + d_2^2 \right) \right] \Delta_{2n}^0 - (d_1 d_2)^2 \Delta_{2n-2}^0. \quad (A6)$$

By imposing the condition

$$Y_1 Y_2 = d_1^2 + d_2^2 + 2d_1 d_2 \cos\theta, \quad (A7)$$

where Y_1 and Y_2 are given by Eq. (A4), the above recurrent sequence can be written as

$$\Delta_{2(n+1)}^0 - (2d_1 d_2 \cos\theta)\Delta_{2n}^0 + (d_1 d_2)^2 \Delta_{2(n-1)}^0 = 0, \quad (A8)$$

whose characteristic algebraic equation has the form $u^2 - 2(d_1 d_2 \cos\theta)u + (d_1 d_2)^2 = 0$. It has two solutions of the form $u = d_1 d_2 e^{\pm i\theta}$. The general solution of the recurrent sequence

can be written as $\Delta_{2n}^0 = (d_1 d_2)^n [C_1 e^{-ni\theta} + C_2 e^{ni\theta}]$. Using the expressions for $n = 1$ and $n = 2$, it follows that

$$C_1 = \frac{\frac{\Delta_4^0 e^{i\theta}}{(d_1 d_2)^2} - \frac{\Delta_2^0 e^{2i\theta}}{(d_1 d_2)}}{e^{i\theta} - e^{-i\theta}} \quad (A9)$$

and

$$C_2 = \frac{-\frac{\Delta_4^0 e^{-i\theta}}{(d_1 d_2)^2} + \frac{\Delta_2^0 e^{-2i\theta}}{d_1 d_2}}{e^{i\theta} - e^{-i\theta}}. \quad (A10)$$

Then

$$\frac{\Delta_{2n}^0}{(d_1 d_2)^n} = \frac{\Delta_2^0}{(d_1 d_2)} \left(\frac{e^{(n-2)i\theta} - e^{-(n-2)i\theta}}{e^{i\theta} - e^{-i\theta}} \right) - \frac{\Delta_4^0}{(d_1 d_2)^2} \left(\frac{e^{(n-1)i\theta} - e^{-(n-1)i\theta}}{e^{i\theta} - e^{-i\theta}} \right). \quad (A11)$$

By using $\sin\omega = \frac{e^{i\omega} - e^{-i\omega}}{2i}$ we obtain

$$\frac{\Delta_{2n}^0}{(d_1 d_2)^n} = \frac{\frac{\Delta_2^0}{(d_1 d_2)} \sin(n-2)\theta - \frac{\Delta_4^0}{(d_1 d_2)^2} \sin(n-1)\theta}{\sin\theta}. \quad (A12)$$

From Eq. (A7) we have $\Delta_2^0 = Y_1 Y_2 - d_1^2 = (d_1 d_2)(\frac{\sin 2\theta + \frac{d_2}{d_1}\sin\theta}{\sin\theta})$ and $\Delta_4^0 = (Y_1 Y_2 - d_1^2)^2 - d_2^2 Y_1 Y_2 = (d_1 d_2)^2 (\frac{\sin 3\theta + \frac{d_2}{d_1}\sin 2\theta}{\sin\theta})$, then Eq. (A12) becomes

$$\frac{\Delta_{2n}^0}{(d_1 d_2)^n} = \frac{\sin 2\theta \sin(n-2)\theta - \sin 3\theta \sin(n-1)\theta}{\sin^2\theta} + \left(\frac{d_2}{d_1} \right) \frac{\sin\theta \sin(n-2)\theta - \sin 2\theta \sin(n-1)\theta}{\sin^2\theta}. \quad (A13)$$

Using the trigonometric formula

$$2\sin\eta \sin\zeta = \cos(\eta - \zeta) - \cos(\eta + \zeta) \quad (A14)$$

we get

$$\frac{\Delta_{2n}^0}{(d_1 d_2)^n} = \frac{1}{2\sin^2\theta} ([\cos(n+2)\theta - \cos n\theta] + \frac{d_2}{d_1}[\cos(n+1)\theta - \cos(n-1)\theta]). \quad (A15)$$

Using Eq. (A14) again, we deduce the expression of Δ_{2n}^0 given in Eq. (A3).

For the first formula of Eq. (A3), we have, from Eq. (A5)

$$\Delta_{2n+1}^0 = \frac{\Delta_{2n+2}^0 + d_1^2 \Delta_{2n}^0}{Y_2}. \quad (A16)$$

Applying the second formula of Eq. (A3), we get

$$\Delta_{2n+1}^0 = \frac{\Delta_{2n+2}^0 + d_1^2 \Delta_{2n}^0}{Y_2} = (d_1 d_2)^n \times \frac{d_1 d_2[\sin(n+2)\theta + \sin n\theta] + (d_1^2 + d_2^2)\sin(n+1)\theta}{Y_2 \sin\theta}. \quad (A17)$$

Using the formula

$$2\sin\eta \cos\zeta = \sin(\eta + \zeta) + \sin(\eta - \zeta) \quad (A18)$$

for $\eta = (n+1)\theta$ and $\zeta = \theta$, we deduce

$$\Delta_{2n+1}^0 = (d_1 d_2)^n \frac{\left[\left(d_1^2 + d_2^2 + 2d_1 d_2 \cos\theta\right)\sin(n+1)\theta\right]}{Y_2 \sin\theta}.$$

(A19)

$$\lambda_k = \left\{ b_1, \frac{(b_1 + b_2) \pm \sqrt{(b_1 - b_2)^2 + 4\left(d_1^2 + d_2^2 + 2d_1 d_2 \cos\frac{k\pi}{n+1}\right)}}{2} \text{ for } k = 1, \ldots, n \right\}$$

(A20)

when $N = 2n + 1$, and

$$\lambda_k = \frac{(b_1 + b_2) \pm \sqrt{(b_1 - b_2)^2 + 4\left(d_1^2 + d_2^2 + 2d_1 d_2 \cos\theta_k\right)}}{2}$$

(A21)

for $k = 1, \ldots, n$ when $N = 2n$. Here, θ_k are the solutions of

$$\sin(n+1)\theta_k + \frac{d_2}{d_1}\sin(n\theta_k) = 0 \qquad (A22)$$

when $N = 2n$. Their validity can be checked explicitly.

APPENDIX B: SPECIAL CASES

1. Alternating masses

A harmonic lattice with alternating masses corresponds to the case where $D_j = D$ and $K_j = K$ for all j and the masses appear as $m_1, m_2, m_1, m_2, \ldots$. The techniques presented in Ref. [10] can be generalized to solve this case [16]. However, we present an alternative derivation as explained in the main text. For the alternating mass lattice, it is based on a technique presented in Ref. [18]. First we impose the following condition

$$\alpha_1 \alpha_2 = 4K^2 \cos^2\left(\frac{q}{2}\right) = 2K^2[\cos(q) + 1]. \qquad (B1)$$

This relation guarantees the consistency of the recursion relation for the characteristic polynomial of Φ in Eq. (4). In the thermal conduction problem, Eq. (B1) determines the conduction band of waves that can propagate through the lattice. Since the masses are alternating, we use the mass-weighted coordinates $\bar{x}_j = \sqrt{m_j}x_j$ to rewrite the equations of motion, which then possess a matrix eigenvalue problem discussed in Appendix A.

Using the results of Ref. [18] and transforming back to the original coordinates, the determinant of Φ can be explicitly written down. If the lattice consists of $N = 2n$ sites, it follows that

$$K_{1,N} = K^{2n}\frac{\sin[(n+1/2)q]}{\sin(q/2)},$$

$$K_{2,N-1} = K^{2n-2}\frac{\sin[(n-1/2)q]}{\sin(q/2)},$$

$$K_{1,N-1} = K^{2(n-1)}\frac{\alpha_1 \sin(nq)}{\sin(q)},$$

$$K_{2,N} = K^{2(n-1)}\frac{\alpha_2 \sin(nq)}{\sin(q)}. \qquad (B2)$$

Then from Eq. (A7), we get the first formula of Eq. (A3) and complete the proof.

Furthermore, the eigenvalues of the class of matrices A_N are given by

Moreover, $|C_{1N}|^2 = K^{4n-2}$. Eq. (3) then becomes

$$\kappa = \frac{\gamma_L \gamma_R}{\pi K^2}\int\frac{d\omega\omega^2}{\mathcal{M}}. \qquad (B3)$$

The domain of the integral is determined by Eq. (B1) and

$$\mathcal{M} = \left[\left(1 - \frac{\gamma_L\gamma_R\omega^2}{K^2}\right)\frac{\cos(q/2)}{\sin(q/2)}\sin(nq)\right.$$
$$\left. + \left(1 + \frac{\gamma_L\gamma_R\omega^2}{K^2}\right)\cos(nq)\right]^2$$
$$+ \left[\frac{\omega}{K^2\sin(q)}(\gamma_R\alpha_1 + \gamma_L\alpha_2)\right]^2\sin^2(nq). \quad (B4)$$

In the limit $n \to \infty$, we follow Ref. [10] and treat nq as an independent variable running from 0 to 2π. Eq. (18) leads to

$$\kappa = \frac{2\gamma_L\gamma_R}{\pi}\int_\Omega d\omega|\omega\sin(q)|$$
$$\times [(1 + \gamma_L\gamma_R\omega^2/K^2)|\gamma_R\alpha_1 + \gamma_L\alpha_2|]^{-1}. \quad (B5)$$

The domain Ω only includes positive ω. This expression recovers the known result in Refs. [10,16].

One may want to check if this reduces to the case of a uniform lattice in the limit $m_1 \to m_2$. When $m_1 = m_2 = m$, $\alpha_1 = \alpha_2 = \alpha$ and Eq. (B1) gives $\alpha = 2K\cos(q/2)$. If we define $\bar{q} = q/2$ and let $\gamma_L = \gamma_R = \gamma$, one can see that

$$\kappa = \frac{\gamma}{\pi K}\int_\Omega d\omega|\omega\sin(\bar{q})|\left(1 + \frac{\gamma^2\omega^2}{K^2}\right)^{-1}. \qquad (B6)$$

This reproduces the result for a uniform harmonic lattice [10].

2. Alternating bonds

Next we consider a harmonic lattice with identical on-site parameters m and D so that $\alpha = D + K_1 + K_2 - m\omega^2$. For convenience, the length of the lattice is $N = 2n + 1$ so that the alternating bonds are in pairs. We will use the results of Ref. [17] for solving this problem.

By imposing the constraint

$$\alpha^2 = K_1^2 + K_2^2 + 2K_1 K_2 \cos(q), \qquad (B7)$$

the propagating modes can be determined. Moreover, the determinant of Φ is given by Ref. [17]. The needed

expressions are

$$K_{1,N} = (K_1 K_2)^n \frac{\alpha \sin[(n+1)q]}{\sin(q)},$$

$$K_{1,N-1} = (K_1 K_2)^n \frac{\sin[(n+1)q] + (K_2/K_1)\sin(nq)}{\sin(q)},$$

$$K_{2,N} = (K_1 K_2)^n \frac{\sin[(n+1)q] + (K_1/K_2)\sin(nq)}{\sin(q)},$$

$$K_{2,N-1} = (K_1 K_2)^{n-1} \frac{\alpha \sin(nq)}{\sin(q)}. \quad \text{(B8)}$$

Moreover, $|C_{1N}|^2 = (K_1 K_2)^{2n}$. Eq. (3) becomes

$$\kappa = \frac{\gamma_L \gamma_R}{\pi} \int d\omega \frac{\omega^2}{\mathcal{B}}. \quad \text{(B9)}$$

Here,

$$\mathcal{B} = \left(\alpha \frac{\sin[(n+1)q]}{\sin(q)} - \frac{\gamma_L \gamma_R \omega^2}{K_1 K_2} \alpha \frac{\sin(nq)}{\sin(q)} \right)^2$$

$$+ \omega^2 \left[\frac{(\gamma_L + \gamma_R)\sin[(n+1)q]}{\sin(q)} \right.$$

$$\left. + \left(\frac{K_1}{K_2}\gamma_L + \frac{K_2}{K_1}\gamma_R \right) \frac{\sin(nq)}{\sin(q)} \right]. \quad \text{(B10)}$$

In the limit $n \to \infty$, we treat nq as an independent variable and integrate from 0 to 2π to average its effect. Then Eq. (23) leads to

$$\kappa = \frac{2\gamma_L \gamma_R}{\pi} \int_\Omega d\omega \frac{|\omega \sin(q)|}{|\alpha|\left[\left(\frac{K_1\gamma_L}{K_2} + \frac{K_2\gamma_R}{K_1} \right) + \frac{(\gamma_L+\gamma_R)\gamma_L\gamma_R\omega^2}{K_1 K_2} \right]}. \quad \text{(B11)}$$

The domain of the integral Ω is determined by Eq. (B7) and only includes positive ω.

We can check if the limit $K_1 \to K_2$ recovers the uniform-lattice result. When $K_1 = K_2 = K$, the constraint, Eq. (B7), becomes $\alpha^2 = 2K^2[1 + \cos(q)] = 4K^2 \cos^2(q/2)$. Thus $\alpha = 2K \cos(q/2)$ and if we define $\tilde{q} = q/2$ and use $\gamma_L = \gamma_R = \gamma$, the thermal conductance becomes

$$\kappa = \frac{\gamma}{\pi K} \int_\Omega d\omega |\omega \sin(\tilde{q})| \left(1 + \frac{\gamma^2 \omega^2}{K^2} \right)^{-1}. \quad \text{(B12)}$$

Again this reduces to the case of a uniform harmonic lattice.

3. Band structure

The band structure of the two special cases are analyzed here. We begin with the alternating-mass case. In this case K is uniform and we have alternating on-site parameters (m_1, D_1) and (m_2, D_2). The constraint Eq. (B1) leads to

$$\cos q = -1 + \frac{1}{2K^2} \{ m_1 m_2 \omega^4 - [m_1(D_2 + 2K)$$

$$+ m_2(D_1 + 2K)]\omega^2 + (D_1 + 2K)(D_2 + 2K)\}. \quad \text{(B13)}$$

Then $|\sin q| = \sqrt{1 - (\cos q)^2}$ will be used in the evaluation of the thermal conductance. The bands are given by the solution

of ω as a function of q. After some algebra we have

$$\omega^2 = \omega_\pm^2 = R_+ \pm \sqrt{R_-^2 + 2\frac{K^2}{m_1 m_2}(\cos q + 1)}. \quad \text{(B14)}$$

Here, $R_\pm = (D_1 + 2K)/(2m_1) \pm (D_2 + 2K)/(2m_2)$. Since only ω^2 is involved in the constraint, for each band with positive ω there is a symmetric band with negative ω. In performing the integral of the conductance, we integrate over the bands with positive ω and add a factor of two to the final result. For positive ω, there are two bands $\omega_{+m} \leqslant \omega \leqslant \omega_{+M}$ and $\omega_{-m} \leqslant \omega \leqslant \omega_{-M}$, where

$$\omega_{+M} = \sqrt{R_+ + \sqrt{R_-^2 + 4\frac{K^2}{m_1 m_2}}},$$

$$\omega_{+m} = \sqrt{2 \max\left(\frac{D_1 + 2K}{2m_1}, \frac{D_2 + 2K}{2m_2} \right)},$$

$$\omega_{-M} = \sqrt{2 \min\left(\frac{D_1 + 2K}{2m_1}, \frac{D_2 + 2K}{2m_2} \right)},$$

$$\omega_{-m} = \sqrt{R_+ - \sqrt{R_-^2 + 4\frac{K^2}{m_1 m_2}}}. \quad \text{(B15)}$$

Then the thermal conductance, Eq. (B5), is readily evaluated by integrating over the two bands.

For the alternating-bond case, the on-site parameters are m and D and they are uniform. The coupling constants are K_1 and K_2. The constraint of Eq. (B7) leads to

$$(D + K_1 + K_2 - m\omega^2)^2$$

$$= (K_1 - K_2)^2 + 2K_1 K_2(\cos q + 1). \quad \text{(B16)}$$

The solution to the constraint gives

$$\omega^2 = \omega_\pm^2 = \frac{1}{m}[(D + K_1 + K_2)$$

$$\pm \sqrt{(K_1 - K_2)^2 + 2K_1 K_2(\cos q + 1)}]. \quad \text{(B17)}$$

For positive frequencies there are two bands $\omega_{+m} \leqslant \omega \leqslant \omega_{+M}$ and $\omega_{-m} \leqslant \omega \leqslant \omega_{-M}$, where

$$\omega_{+M} = \sqrt{\frac{D + 2K_1 + 2K_2}{m}},$$

$$\omega_{+m} = \sqrt{\frac{1}{m} \max(D + 2K_1, D + 2K_2)},$$

$$\omega_{-M} = \sqrt{\frac{1}{m} \min(D + 2K_1, D + 2K_2)},$$

$$\omega_{-m} = \sqrt{\frac{D}{m}}. \quad \text{(B18)}$$

The conductance, Eq. (B11), can be evaluated accordingly.

APPENDIX C: SMALL AND LARGE γ REGIMES

Here we will derive analytic expressions in the limiting regimes. The small γ regime is especially helpful in

understanding the sensitivity of the conductance to changes in configuration, which we will also discuss.

1. Small γ

When N is odd, Eq. (24) gives the device conductance in all regimes. Dropping the higher-order terms in γ yields

$$\kappa = k_B \frac{2\gamma_L\gamma_R}{\pi} \int_\Omega d\omega \frac{|\omega\sin(q)|}{\alpha_1\left(\frac{K_1}{K_2}\gamma_L + \frac{K_2}{K_1}\gamma_R\right)} \tag{C1}$$

$$= k_B \frac{2\gamma_L\gamma_R}{\pi\left(\frac{K_1}{K_2}\gamma_L + \frac{K_2}{K_1}\gamma_R\right)} \int_\Omega d\omega \frac{|\omega\sin(q)|}{D_1 + K_1 + K_2 - m_1\omega^2}.$$

When N is even, the corresponding equation is Eq. (19). Dropping the higher-order terms in γ yields

$$\kappa = k_B \frac{2\gamma_L\gamma_R}{\pi} \frac{K_1}{K_2} \int_\Omega \frac{d\omega|\omega\sin(q)|}{|\gamma_R\alpha_1 + \gamma_L\alpha_2|}. \tag{C2}$$

Both of these integrals have the same form.

Changing variables to momentum, brings the integrals to

$$\frac{1}{\pi}\int dq \frac{A\sin^2 q}{B + C\cos q}. \tag{C3}$$

Integrating separately over each band and adding the results yields

$$\kappa = \frac{2A}{B + \sqrt{B^2 - C^2}}. \tag{C4}$$

For the odd length lattice, we have

$$A = k_B \frac{2\gamma_L\gamma_R K_1 K_2/m_1}{\frac{K_1}{K_2}\gamma_L + \frac{K_2}{K_1}\gamma_R}, \tag{C5}$$

$B = K_1^2 + K_2^2$, and $C = 2K_1K_2$. This yields the conductance (for $K_1 < K_2$)

$$\kappa = \frac{k_B\gamma_L\gamma_R/m_1}{\gamma_L + f^{-2}\gamma_R}, \tag{C6}$$

which is an exact expression in this regime for the odd lattice. As in the main text, $f = K_1/K_2$.

For the even length lattice (and $K_1 < K_2$), the coefficients are

$$A = k_B 2\gamma_L\gamma_R K_1^2(m_2\gamma_L + m_1\gamma_R), \tag{C7}$$

$$B = \gamma_L\gamma_R(D_2'm_1 - D_1'm_2)^2 + (m_2\gamma_L + m_1\gamma_R)^2 K^2, \tag{C8}$$

and

$$C = 2K_1K_2(m_2\gamma_L + m_1\gamma_R)^2, \tag{C9}$$

where $K^2 = K_1^2 + K_2^2$ and $D_i' = D_i + K_1 + K_2$. The resulting expression is complicated. However, as can be seen directly from the integral itself, when swapping K_1 and K_2 to get the conductance in the absence of edge modes, $\bar{\kappa}$, the ratio is

$$\frac{\kappa}{\bar{\kappa}} = \left(\frac{K_1}{K_2}\right)^2. \tag{C10}$$

This equation [and the one for odd lattices, Eq. (C6)] is reflective of the topological origin of the excess resistance seen in Fig. 2. When simply swapping parameters or going from an even to odd length lattice, one introduces edge modes that suppress the coupling between the bulk modes and the external reservoirs.

2. Large γ

When N is odd, Eq. (24) gives the device conductance in all regimes. Dropping the higher-order terms in γ yields

$$\kappa = k_B \frac{2K_1K_2}{\pi(\gamma_L + \gamma_R)} \int_\Omega \frac{d\omega}{\omega}\left|\frac{\sin(q)}{\alpha_2}\right|. \tag{C11}$$

When N is even, the corresponding equation is Eq. (19). Dropping the higher-order terms in γ yields

$$\kappa = k_B \frac{2K_1K_2}{\pi} \int_\Omega \frac{d\omega}{\omega}\left|\frac{\sin(q)}{\gamma_R\alpha_1 + \gamma_L\alpha_2}\right|. \tag{C12}$$

Both of these integrals have the same form.

Changing variables to momentum brings the integrals to

$$\frac{1}{\pi}\int dq \frac{A\sin^2 q}{(B + C\cos q)(B' - C'\cos q)}. \tag{C13}$$

Integrating separately over each band and adding the results yields

$$\kappa = \frac{A}{CC'}\left(1 - \frac{C'\sqrt{B^2 - C^2} + C\sqrt{B'^2 - C'^2}}{B'C + BC'}\right). \tag{C14}$$

For the odd length lattice, we have

$$A = 2K_1^2 K_2^2 D_1', \tag{C15}$$

$$B = K^2, \tag{C16}$$

$$C = 2K_1K_2, \tag{C17}$$

$$B' = D_1'D_2' - K^2, \tag{C18}$$

and

$$C' = 2K_1K_2. \tag{C19}$$

This yields (for $K_1 < K_2$)

$$\kappa = \frac{D_1'D_2' - \sqrt{(D_1'D_2' - K^2)^2 - 4K_1^2K_2^2} + K_1^2 - K_2^2}{D_2'(\gamma_L + \gamma_R)/2}. \tag{C20}$$

For the even length lattice, we have

$$A = 2K_1^2 K_2^2\left(D_1'm_2^2\gamma_L + D_2'm_1^2\gamma_R\right), \tag{C21}$$

$$B = (D_2'm_1 - D_1'm_2)^2\gamma_L\gamma_R + (m_2\gamma_L + m_1\gamma_R)^2 K^2, \tag{C22}$$

$$C = 2K_1K_2(m_2\gamma_L + m_1\gamma_R)^2, \tag{C23}$$

$$B' = D_1'D_2' - K^2, \tag{C24}$$

and

$$C' = 2K_1K_2. \tag{C25}$$

3. Uniform lattice in these regimes

For a uniform lattice coupled to two reservoirs with couplings γ_L and γ_R, we can obtain its expression from those of alternating lattices. Explicitly, $\alpha = D + 2K - m\omega^2 = 2K\cos\tilde{q}$ with $\tilde{q} = q/2$ and

$$\kappa = k_B \frac{2\gamma_L\gamma_R}{\pi} \int_\Omega d\omega \frac{|\omega\sin q|}{(\gamma_L + \gamma_R)\alpha\left(1 + \frac{\gamma_L\gamma_R}{K_1 K_2}\omega^2\right)}. \quad (C26)$$

In the limit $\gamma_L,\gamma_R \to 0$, using $\omega d\omega = (K/m)\sin(\tilde{q})d\tilde{q}$ and $\sin(q) = 2\sin(\tilde{q})\cos(\tilde{q})$ one obtains

$$\kappa \to k_B \frac{\gamma_L\gamma_R}{\pi(\gamma_L + \gamma_R)} \int_0^{2\pi} d\tilde{q} \frac{K\sin^2\tilde{q}}{m}$$

$$= \frac{\gamma_L\gamma_R}{(\gamma_L + \gamma_R)}\left(\frac{k_B}{m}\right). \quad (C27)$$

This analysis also applies to a uniform lattice with different γ_L and γ_R in the large γ regime, where we have

$$\kappa \to k_B \frac{2\gamma_L\gamma_R}{\pi} \int_\Omega \frac{d\omega|\omega\sin q|}{(\gamma_L + \gamma_R)\alpha\frac{\gamma_L\gamma_R}{K^2}\omega}$$

$$= \frac{k_B K^2}{\pi(\gamma_L + \gamma_R)} \int_0^{2\pi} \frac{\frac{K}{m}d\tilde{q}\sin\tilde{q}(2\sin\tilde{q}\cos\tilde{q})}{(2K\cos\tilde{q})\frac{1}{m}(D + 2K - 2K\cos\tilde{q})}$$

$$= k_B \frac{K}{(\gamma_L + \gamma_R)}\left(1 - \frac{\sqrt{D(D+4K)}}{2K} + \frac{D}{2K}\right). \quad (C28)$$

When $\gamma_L = \gamma_R = \gamma$, those expressions recover Eqs. (25) and (C31).

4. Compact expressions for special choices of γ's

For the case of $N = 2n$, $\gamma_L = \Lambda m_1$ and $\gamma_R = \Lambda m_2$, an analytic expression for κ in the small γ regime (corresponding to $\Lambda \to 0$) can be found from the full expression of Eq. (19). In this limit,

$$\kappa \to k_B \frac{2\Lambda m_1 m_2}{\pi} \int_\Omega \frac{d\omega\omega|\sin(q)|}{(m_2\alpha_1 + m_1\alpha_2)(K_2/K_1)}. \quad (C29)$$

From the constraint, Eq. (9), which leads to the band structure, we obtain $\omega d\omega = K_1 K_2 \sin(q)dq/(m_1\alpha_2 + m_2\alpha_1)$. Moreover, using $\alpha_1\alpha_2 = K_1^2 + K_2^2 + 2K_1 K_2\cos q$, $m_2\alpha_1 - m_1\alpha_2 = m_2(D_1 + K_1 + K_2) - m_1(D_2 + K_1 + K_2) \equiv \mathcal{M}$, and defining $\nu \equiv \mathcal{M}^2/(m_1 m_2) + 4(K_1^2 + K_2^2)$, one can use the fact that

$\mathcal{M}$ and ν are independent of ω to obtain

$$\kappa = k_B \frac{2\Lambda K_1^2}{\pi} \int_0^{2\pi} dq \frac{\sin^2(q)}{\nu + 8K_1 K_2\cos(q)}$$

$$= k_B \Lambda \frac{(\nu - \sqrt{\nu^2 - 64K_1^2 K_2^2})}{16K_2^2}. \quad (C30)$$

Thus κ is linear in the friction coefficient, as expected.

For a uniform harmonic lattice in the large γ limit, the thermal conductance takes the form [19]

$$\kappa \to k_B \frac{K}{2\gamma}\left(1 - \frac{\sqrt{mD}}{2K}\Omega\right). \quad (C31)$$

The bandwidth for the uniform lattice is $\Omega = \frac{K}{m}(\sqrt{D/K + 4} - \sqrt{D/K})$.

When N is even, Eq. (19) allows a compact expression in the large γ regime. Similar to the small γ expansion, we choose $\gamma_L = \Lambda m_1$ and $\gamma_R = \Lambda m_2$, where Λ is the large parameter. The leading term in the thermal conductance becomes

$$\kappa \to k_B \frac{2\Lambda m_1 m_2}{\pi} \int_\Omega \frac{d\omega|\omega\sin q|}{(m_2\alpha_1 + m_1\alpha_2)\frac{\Lambda^2 m_1 m_2}{K_1 K_2}\omega^2}. \quad (C32)$$

The simplification is similar to that in the small γ calculation. $\omega d\omega = K_1 K_2\sin qdq/(m_2\alpha_1 + m_1\alpha_2)$. Moreover, $(m_1\alpha_2 + m_2\alpha_1)^2 = m_1 m_2(\nu + 8K_1 K_2\cos q)$, where $\nu = \mathcal{M}^2/(m_1 m_2) + 4(K_1^2 + K_2^2)$ and $\mathcal{M} = m_2(D_1 + K_1 + K_2) - m_1(D_2 + K_1 + K_2)$. We also solve Eq. (9) to get $\omega_\pm^2 = (\mathcal{A} \pm \mathcal{B})/(2m_1 m_2)$, where $\mathcal{A} = m_2(D_1 + K_1 + K_2) + m_1(D_2 + K_1 + K_2)$ and $\mathcal{B} = \sqrt{\mathcal{M}^2 + 4m_1 m_2\alpha_1\alpha_2}$. The two solutions of ω^2 correspond to the two bands and we need to integrate over both bands. The identity $1/\omega_+^2 + 1/\omega_-^2 = 4m_1 m_2\mathcal{A}/(\mathcal{A}^2 - \mathcal{B}^2)$ helps the merge of the integrations over the two bands. By defining $\rho = 4[2K_1 K_2 + D_1 D_2 + (D_1 + D_2)(K_1 + K_2)]$, $\mathcal{A}^2 - \mathcal{B}^2 = m_1 m_2(\rho - 8K_1 K_2\cos q)$. The thermal conductance becomes

$$\kappa = k_B \frac{K_1^2 K_2^2}{\Lambda\pi} \frac{4\mathcal{A}}{m_1 m_2} \int_0^{2\pi} dq \sin^2(q)[(\nu - 8K_1 K_2\cos q)$$

$$\times (\rho - 8K_1 K_2\cos q)]^{-1}$$

$$= \frac{k_B}{\Lambda} \frac{\mathcal{A}}{8m_1 m_2(\nu + \rho)}[\nu + \rho$$

$$- \sqrt{(\nu + 8K_1 K_2)(\nu - 8K_1 K_2)}$$

$$- \sqrt{(\rho + 8K_1 K_2)(\rho - 8K_1 K_2)}]. \quad (C33)$$

For a uniform lattice with $\gamma = \Lambda m$, this expression fully recovers Eq. (C31).

[1] A. Dhar, Phys. Rev. Lett. **86**, 5882 (2001).

[2] S. Lepri, R. Livi, and A. Politi, Phys. Rep. **377**, 1 (2003).

[3] Y. Dubi and M. Di Ventra, Rev. Mod. Phys. **83**, 131 (2011).

[4] G. Chen, *Nanoscale Energy Transport and Conversion: A Parallel Treatment of Electrons, Molecules, Phonons, and Photons* (Oxford University Press, Oxford, 2005).

[5] T. S. Fisher, *Thermal Energy at the Nanoscale* (World Scientific, Singapore, 2014).

[6] N. Li, J. Ren, L. Wang, G. Zhang, P. Hänggi, and B. Li, Rev. Mod. Phys. **84**, 1045 (2012).

[7] L. Wang and B. Li, Phys. Rev. Lett. **101**, 267203 (2008).

[8] K. A. Velizhanin, C. C. Chien, Y. Dubi, and M. Zwolak, Phys. Rev. E **83**, 050906(R) (2011).

[9] C. C. Chien, K. A. Velizhanin, Y. Dubi, and M. Zwolak, Nanotech. **24**, 095704 (2013).

[10] A. Casher and J. L. Lebowitz, J. Math. Phys. **12**, 1701 (1971).

[11] G. Weber, J. W. Essex, and C. Neylon, Nat. Phys. **5**, 769 (2009).

[12] B. S. Alexandrov, V. Gelev, Y. Monisova, L. B. Alexandrov, A. R. Bishop, K. Ø. Rasmussen, and A. Usheva, Nucl. Acids Res. **37**, 2405 (2009).

[13] B. van Grinsven, N. V. Bon, H. Trauven, L. Grieten, M. Murib, K. L. Jimenez Monroy, S. D. Janssens, K. Haenen, M. J. Schoning, V. Vermeerne, M. Ameloot, L. Michiels, R. Thoelen, W. De Ceuninck, and P. Wagner, ACS Nano **6**, 2712 (2012).

[14] Z. Xu, X. Wang, and H. Xie, Polymer **55**, 6373 (2014).

[15] E. Pereira, L. M. Santana, and R. Avila, Phys. Rev. E **84**, 011116 (2011).

[16] V. Kannan, A. Dhar, and J. L. Lebowitz, Phys. Rev. E **85**, 041118 (2012).

[17] S. Kouachi, Electron. J. Linear Algebra **15**, 115 (2006).

[18] S. Kouachi, Appl. Math. (Warsaw) **35**, 107 (2008).

[19] K. A. Velizhanin, S. Sahu, C.-C. Chien, Y. Dubi, and M. Zwolak, Sci. Rep. **5**, 17506 (2015).

[20] C. C. Chien, K. A. Velizhanin, Y. Dubi, B. R. Ilic, and M. Zwolak (unpublished).

[21] I. S. Gradshteyn and I. M. Ryzhik, *Table of Integrals, Series, and Products*, 7th ed., edited by A. Jeffrey and D. Zwillinger (Academic Press, Burlington, USA, 2007).

[22] H. Matsuda and K. Ishii, Prog. Theor. Phys. Suppl. **45**, 56 (1970).

[23] G. Theocharis, N. Boechler, P. G. Kevrekidis, S. Job, M. A. Porter, and C. Daraio, Phys. Rev. E **82**, 056604 (2010).

[24] A. Franchini, V. Bortolani, and R. F. Wallis, J. Phys.: Condens. Matter **14**, 145 (2002).

[25] E. Pereira, H. C. F. Lemos, and R. R. Avila, Phys. Rev. E **84**, 061135 (2011).

[26] E. Pereira and H. C. F. Lemos, Phys. Rev. E **78**, 031108 (2008).

[27] E. Pereira and H. C. F. Lemos, J. Phys. A: Math. Theor. **42**, 225006 (2009).

[28] D. Segal, Phys. Rev. E **79**, 012103 (2009).

[29] J. F. Elliott, Masters Thesis, University of Tennessee, 1953 (unpublished).

[30] U. Grenander and G. Szego, *Toeplitz Forms and Their Applications* (University of California Press, Berkeley, 1958).

[31] W. C. Yueh, App. Math. E-Notes **5**, 66 (2005).

[32] R. T. Gregory and D. Carney, *A Collection of Matrices for Testing Computational Algorithms* (Wiley-Interscience, New York, 1969).